

Role of graphene oxide (GO) nanosheet sizes, pinhole defects and non-ideal lamellar stacking on the performance of layered GO membranes: An atomistic investigation

Abhijit Gogoi, Aditya Koneru, and K. Anki Reddy*

E-mail: anki.reddy@iitg.ac.in

OPLS-AA Force Field

In OPLS-AA force field¹ the following bonded interactions are considered.

- Bond Stretching

$$V_b(r_{ij}) = k_{ij}^b (r_{ij} - b_0)^2 \quad (1)$$

The bond stretching interaction between atoms i, j is given by $V_b(r_{ij})$ which is modeled through Eq. 1. Here b_0 is the equilibrium bond distance between atoms i, j and r_{ij} is the instantaneous bond distance between them. k_{ij}^b is the spring constant of the bond between i and j .

- Bond-angle bending

$$V_a(\theta_{ijk}) = k_{i,j,k}^\theta (\theta_{ijk} - \theta_{ijk}^0)^2 \quad (2)$$

The bond-angle bending interaction $V_a(\theta_{ijk})$ between the three atoms i , j and k which are bonded through two bonds is given by Eq. 2. θ_{ijk} is the instantaneous bond angle between i , j , k with j being the central atom. θ_{ijk}^0 is the equilibrium bond angle and $k_{i,j,k}^\theta$ is the corresponding force constant.

- Torsional Interaction

$$V_d(\phi_{ijkl}) = \frac{V_1}{2} [1 + \cos(\phi + f_1)] + \frac{V_2}{2} [1 - \cos(2\phi + f_2)] + \frac{V_3}{2} [1 + \cos(3\phi + f_3)] \quad (3)$$

The torsional interaction $V_d(\phi_{ijkl})$ due to the torsional angle ϕ_{ijkl} between the planes containing the atoms with indices i, j, k and j, k, l is given by Eq. 3 where V_i , ($i = 1, 2, 3...$) is the corresponding Fourier coefficients for torsional energy functions.

The non-bonded interactions in the present simulation are van der Waals interaction and Coulomb interaction.

- van der Waals interaction

$$V_{\text{LJ}}(r_{ij}) = \frac{C_{ij}^{(12)}}{r_{ij}^{(12)}} - \frac{C_{ij}^{(6)}}{r_{ij}^{(6)}} \quad (4)$$

In this present work the van der Waals interaction is modeled through Lennard-Jones (LJ) potential given by Eq. 4. The parameters $C_{ij}^{(12)} = 4\epsilon_{ij}\sigma_{ij}^{(12)}$ and $C_{ij}^{(6)} = 4\epsilon_{ij}\sigma_{ij}^{(6)}$ depend

on the pair of atom types. For the interactions with different atom types the following combination rules are applied

$$C_{ij}^{(6)} = \left(C_{ii}^{(6)} C_{jj}^{(6)} \right)^{1/2} \quad (5)$$

$$C_{ij}^{(12)} = \left(C_{ii}^{(12)} C_{jj}^{(12)} \right)^{1/2} \quad (6)$$

$$\epsilon_{ij} = \left(\epsilon_{ii} \epsilon_{jj} \right)^{1/2} \quad (7)$$

$$\sigma_{ij} = \left(\sigma_{ii} \sigma_{jj} \right)^{1/2} \quad (8)$$

In the above expression ϵ_{ij} is the potential well depth and σ_{ij} is the distance where potential equals zero.

- Coulomb interaction

$$V_C(r_{ij}) = \frac{1}{4\pi\epsilon_0} \frac{q_i q_j}{\epsilon_r r_{ij}} \quad (9)$$

Here ϵ_0 and ϵ_r are the vacuum and relative dielectric permittivities, respectively.

GO nanosheet

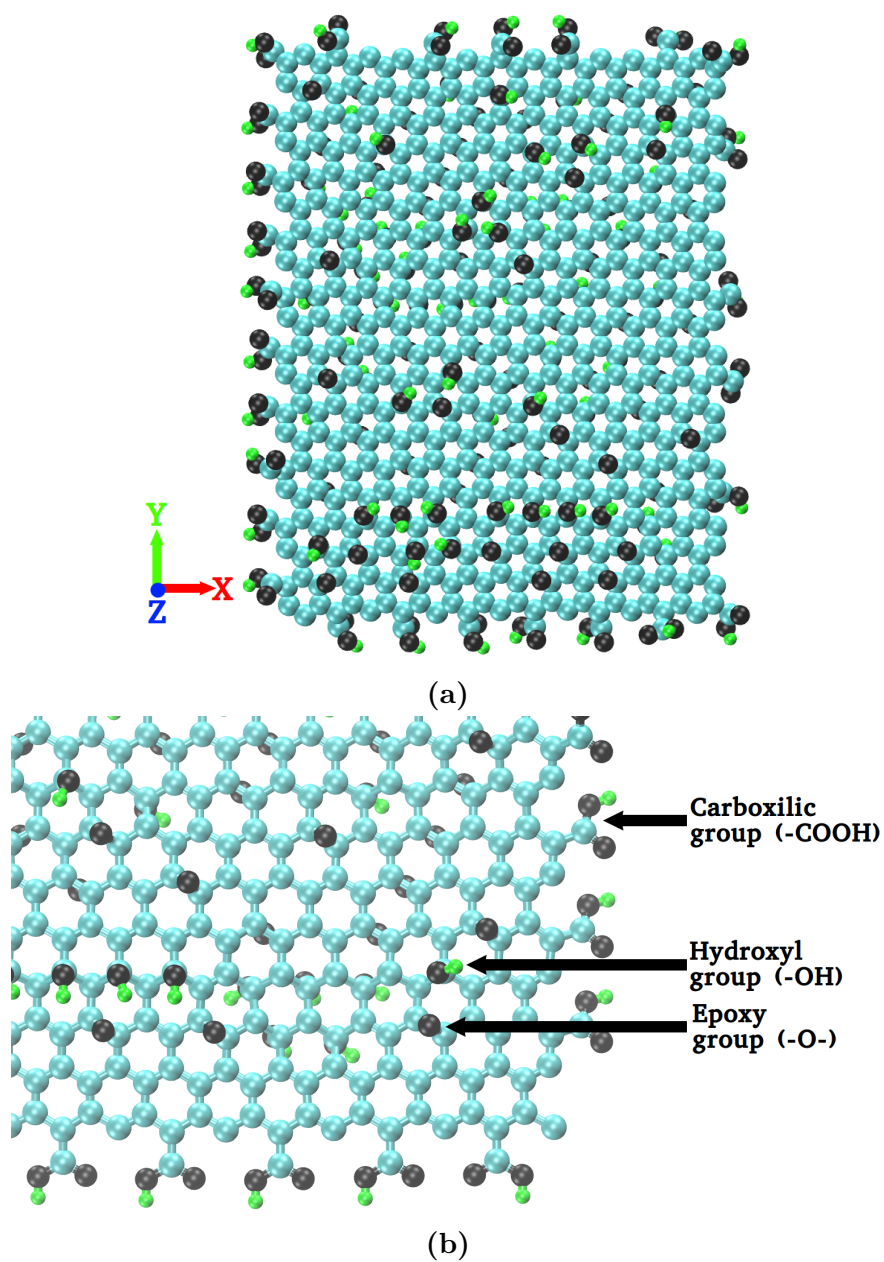


Fig. S1. (a) GO nanosheet. (b) The distribution of functional groups on GO nanosheet. The green color is for hydrogen atoms, the black color is for oxygen atoms and the cyan color is for carbon atoms.

Hydrated layered GO membrane with non-ideal lamellar stacking

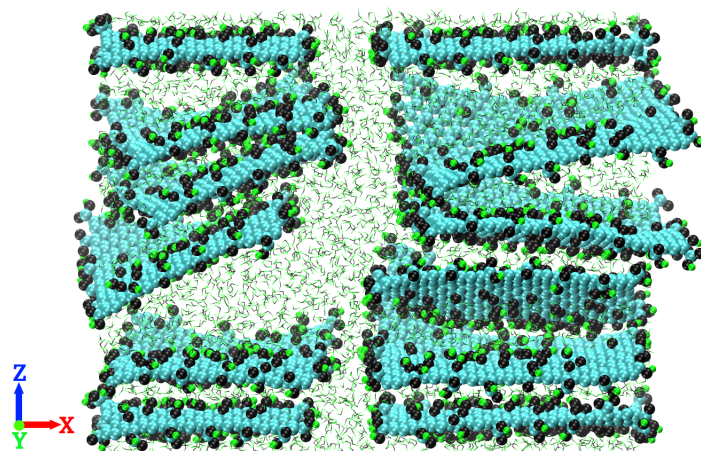


Fig. S2. Hydrated layered GO membrane of configuration 0-NP-nIL.

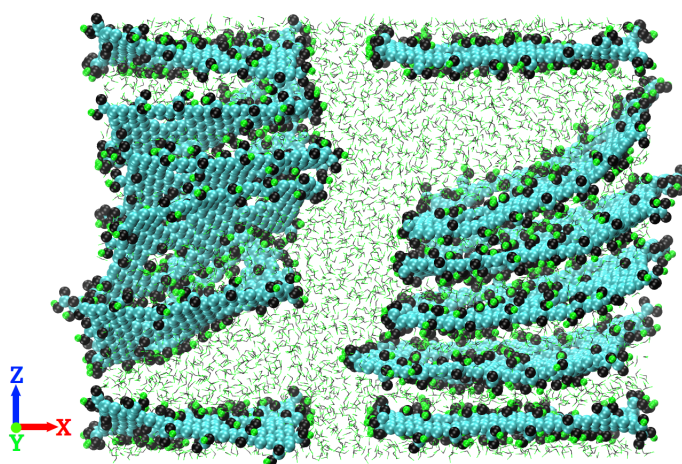


Fig. S3. Hydrated layered GO membrane of configuration 0-P-nIL.

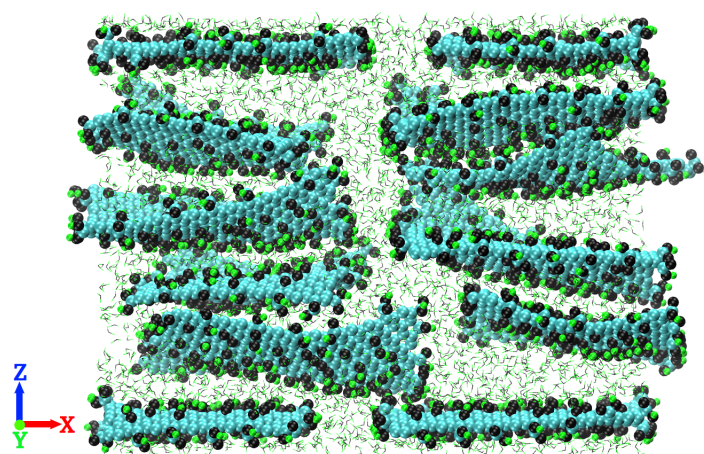


Fig. S4. Hydrated layered GO membrane of configuration 8-NP-nIL.

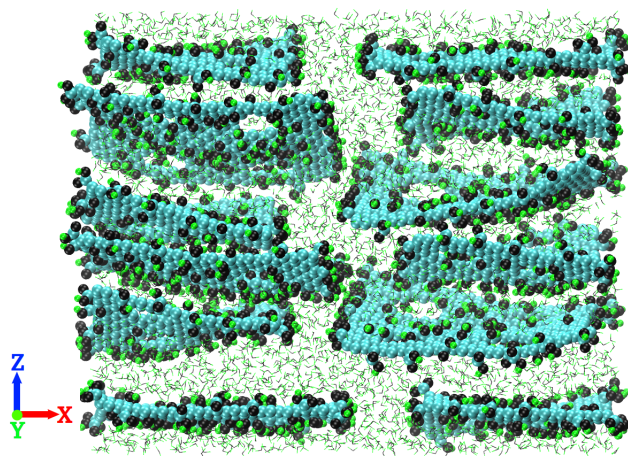


Fig. S5. Hydrated layered GO membrane of configuration 8-P-nIL.

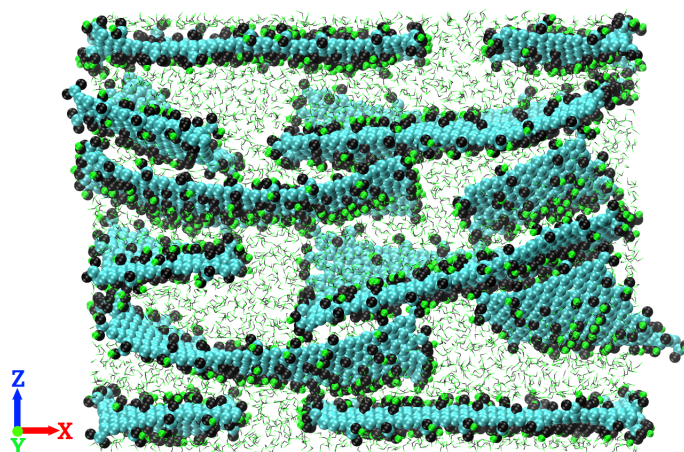


Fig. S6. Hydrated layered GO membrane of configuration 24-NP-nIL.

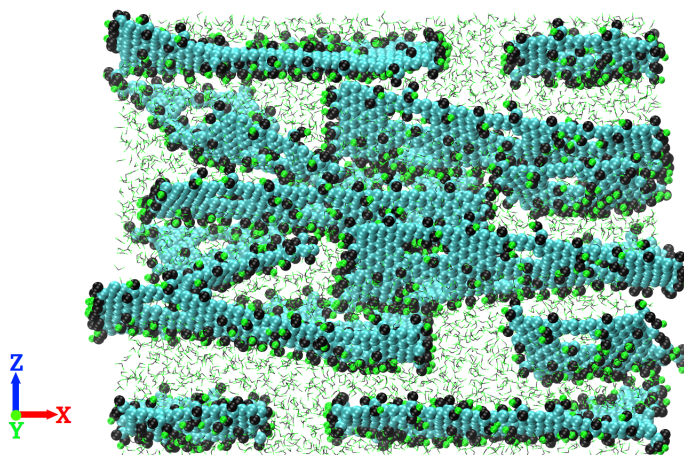


Fig. S7. Hydrated layered GO membrane of configuration 24-P-nIL.

Ion permeation events

Table S1: Ion permeation events through layered GO membranes.

Membrane	Ion permeation events
0-NP-IL	5
0-P-IL	8
8-NP-IL	0
8-P-IL	3
24-NP-IL	0
24-P-IL	0
0-NP-nIL	5
0-P-nIL	11
8-NP-nIL	0
8-P-nIL	1
24-NP-nIL	0
24-P-nIL	0

Trajectory of water molecules through layered GO membranes with non-ideal lamellar stacking

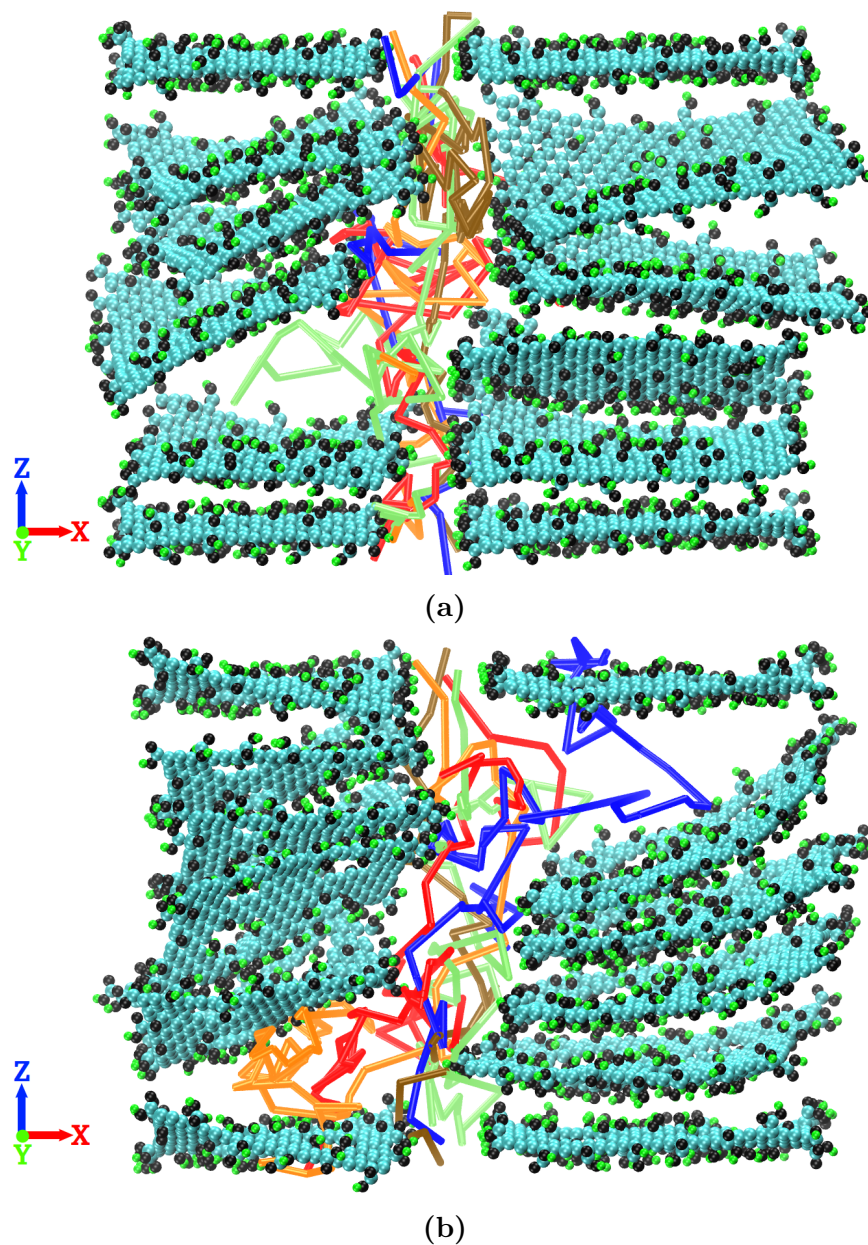
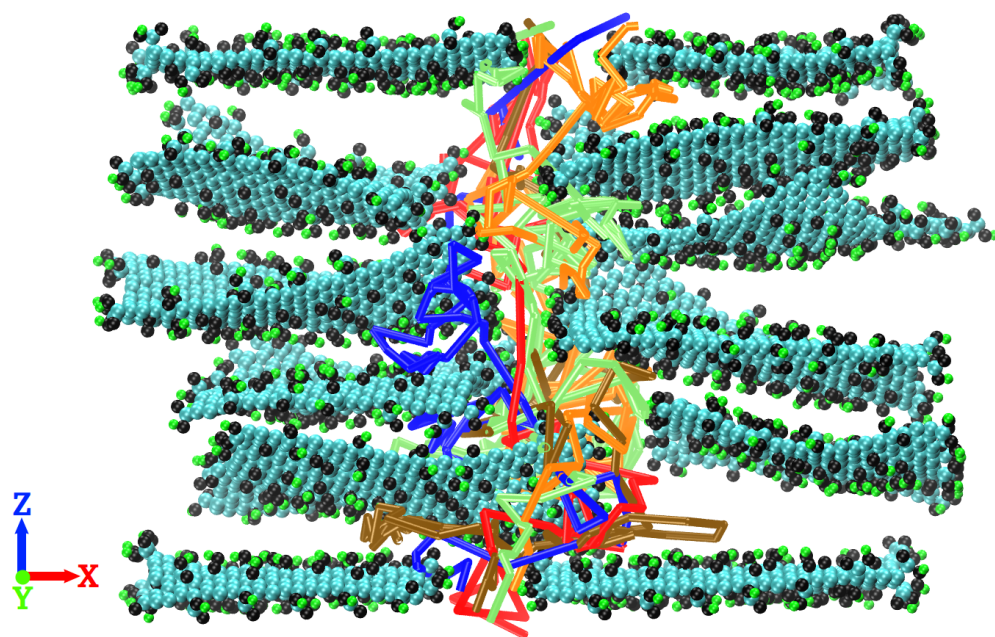
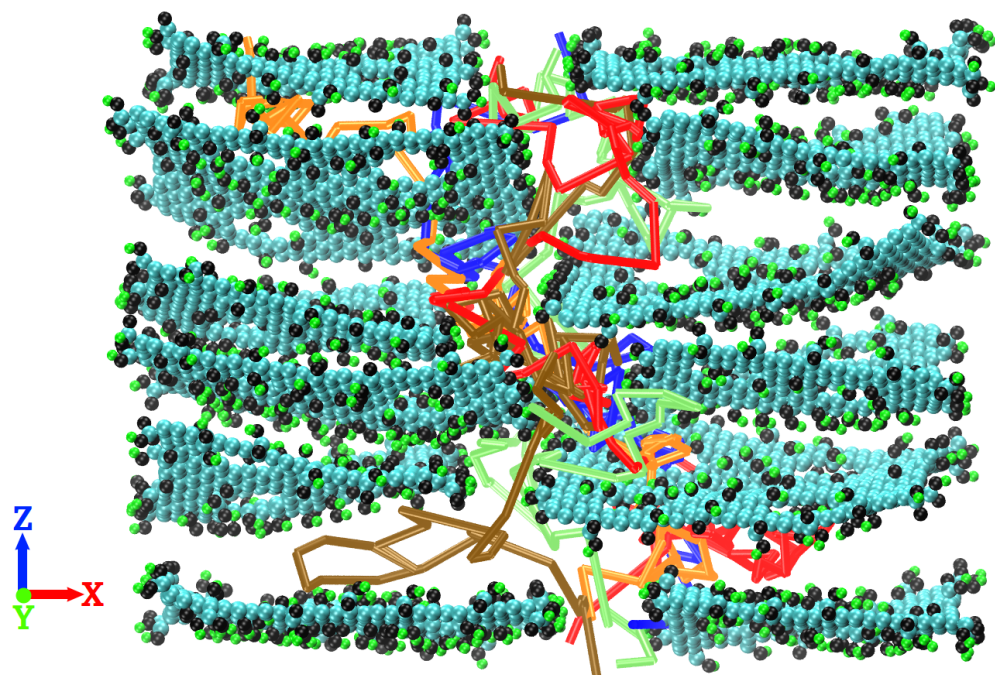


Fig. S8. Trajectory of permeating water molecules through layered GO membranes (a) 0-NP-nIL, (b) 0-P-nIL.

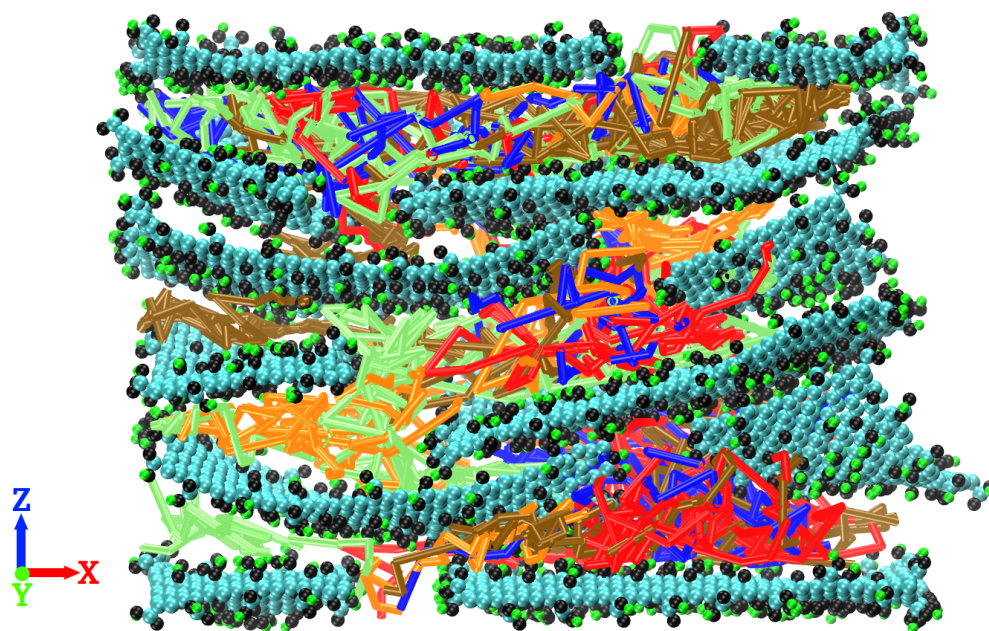


(a)

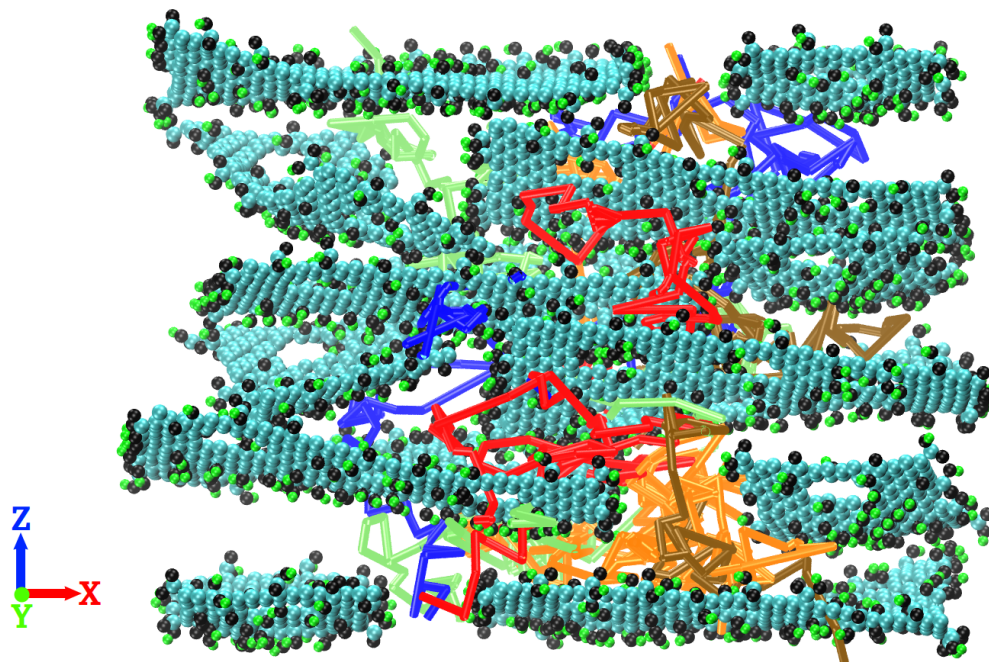


(b)

Fig. S9. Trajectory of permeating water molecules through layered GO membranes (a) 8-NP-nIL, (b) 8-P-nIL.



(a)



(b)

Fig. S10. Trajectory of permeating water molecules through layered GO membranes (a) 24-NP-nIL, (b) 24-P-nIL.

Trajectory of ions inside the layered GO membranes

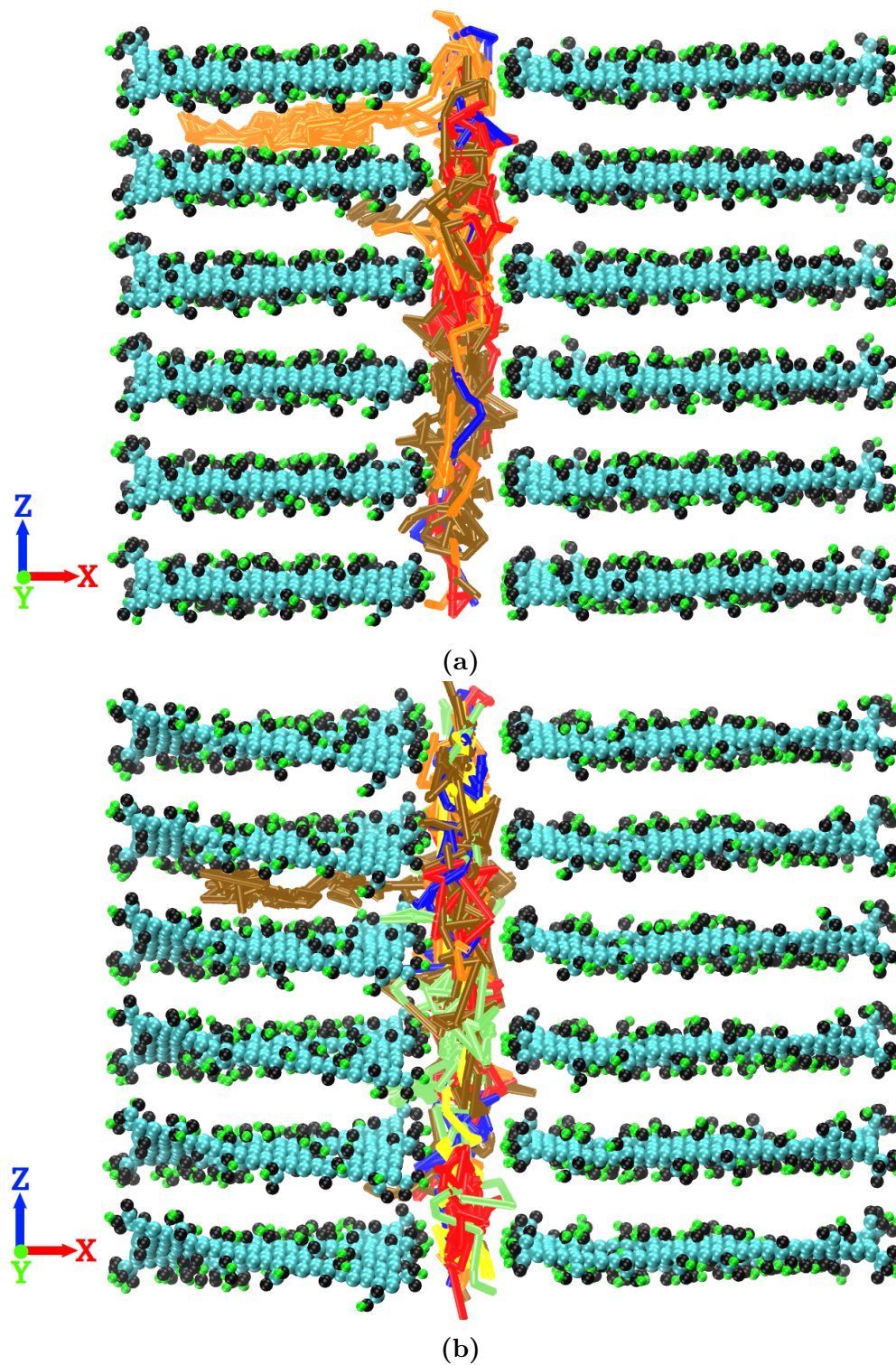


Fig. S11. Trajectory of Cl^- ions through layered GO membranes (a) 0-NP-IL, (b) 0-P-IL.

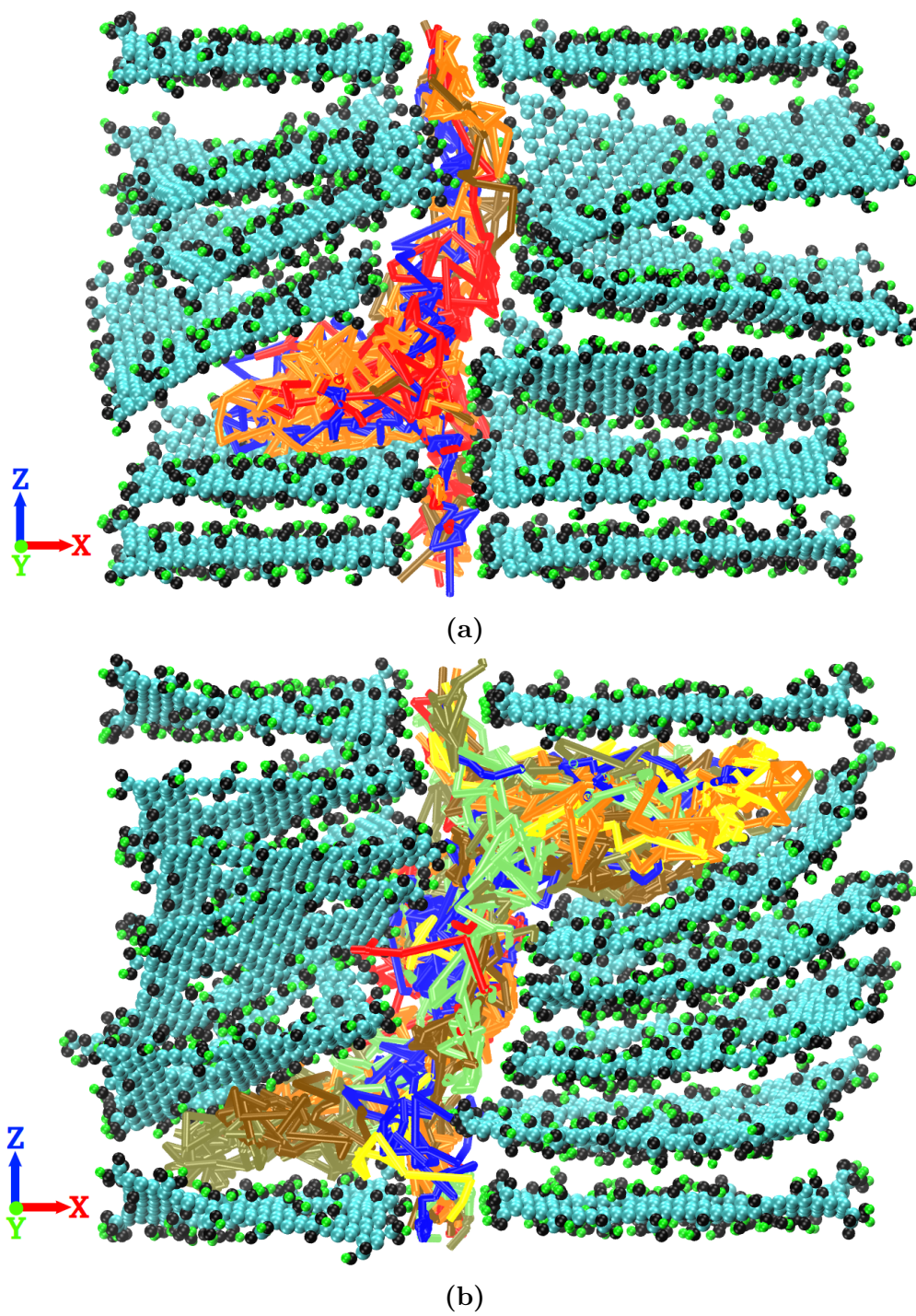
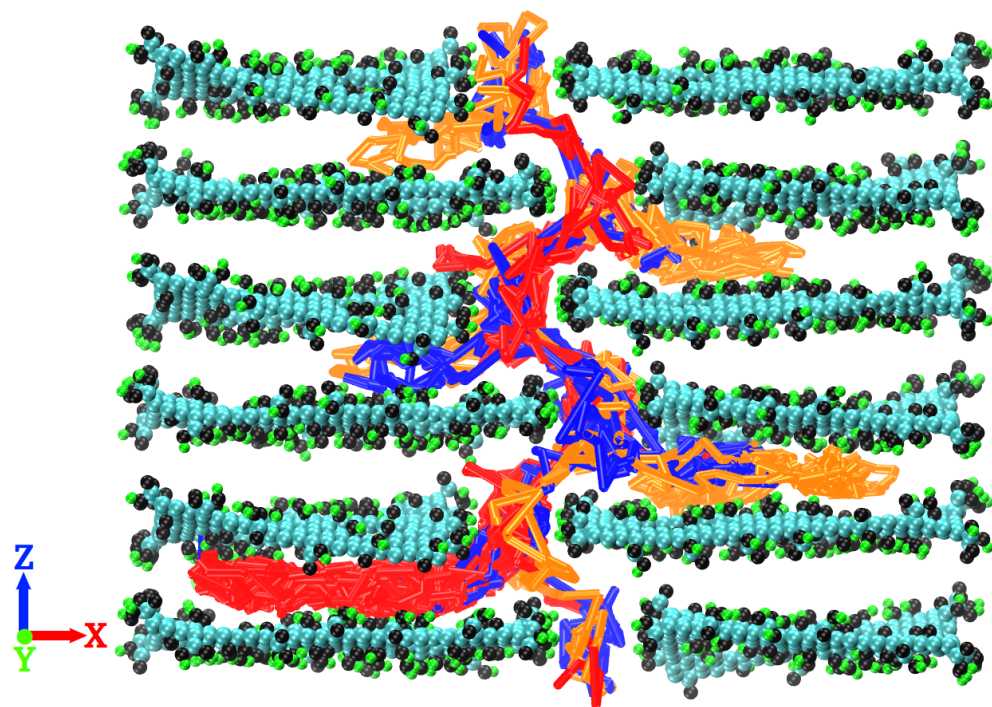
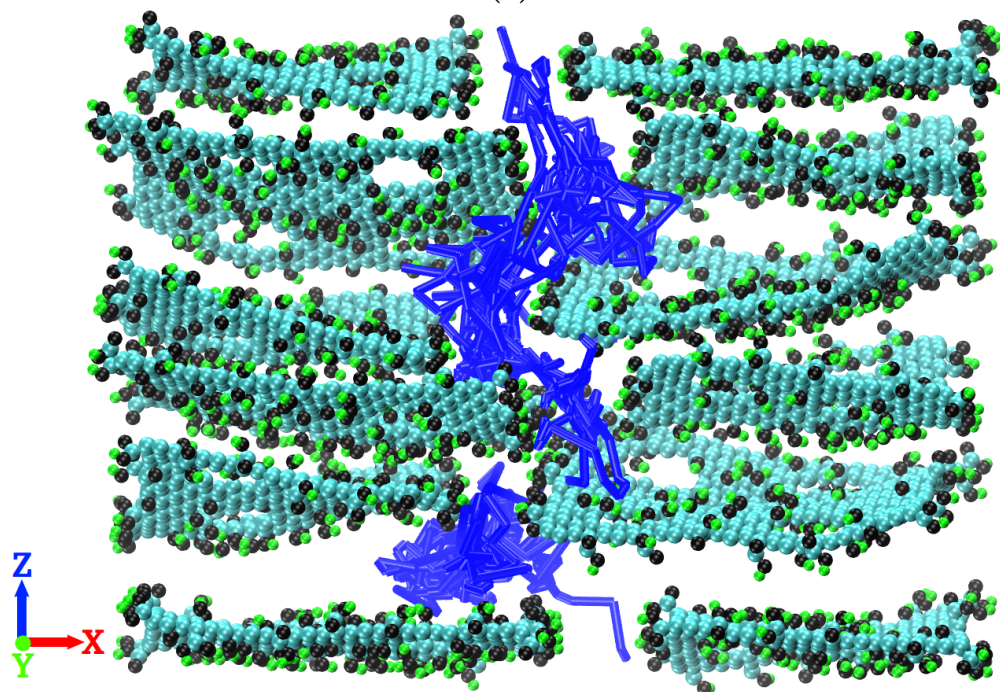


Fig. S12. Trajectory of Cl^- ions through layered GO membranes (a) 0-NP-nIL, (b) 0-P-nIL.

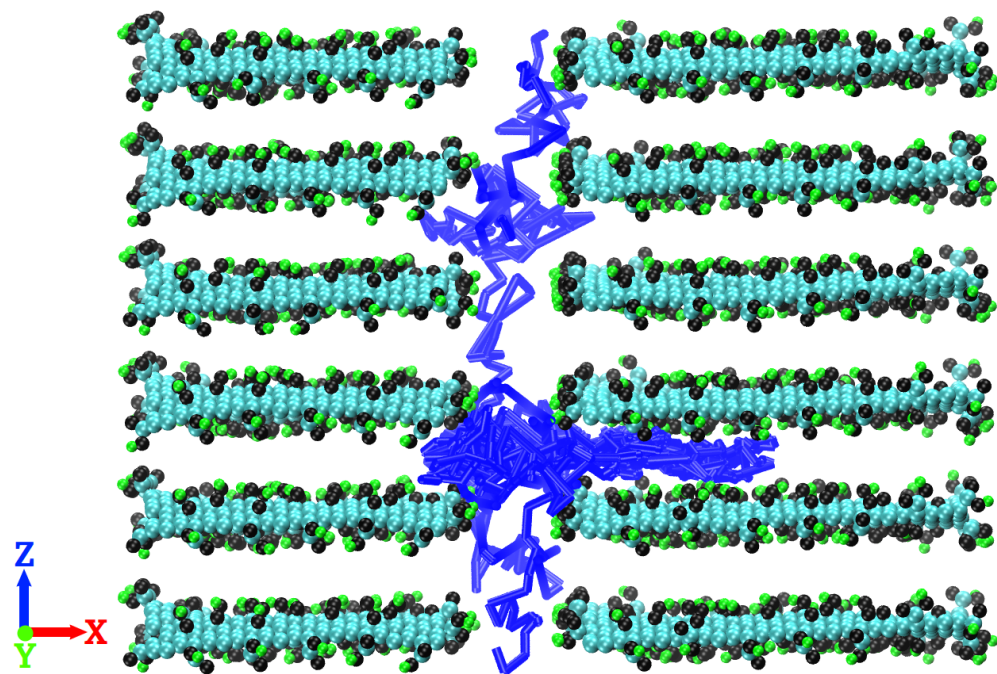


(a)

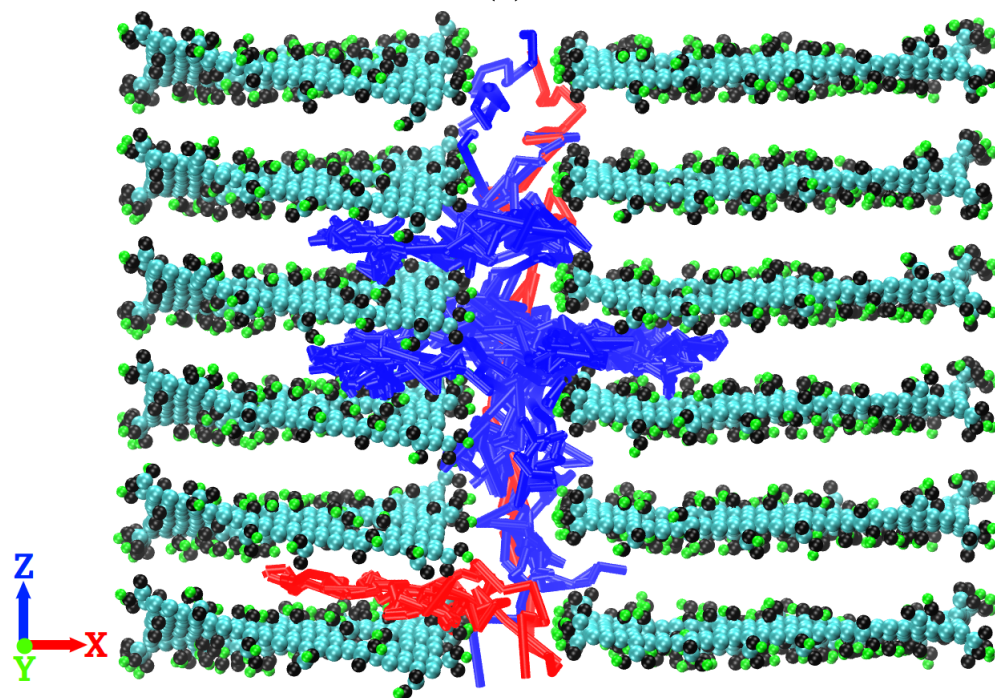


(b)

Fig. S13. Trajectory of Cl^- ions through layered GO membranes (a) 8-P-IL, (b) 8-P-nIL.

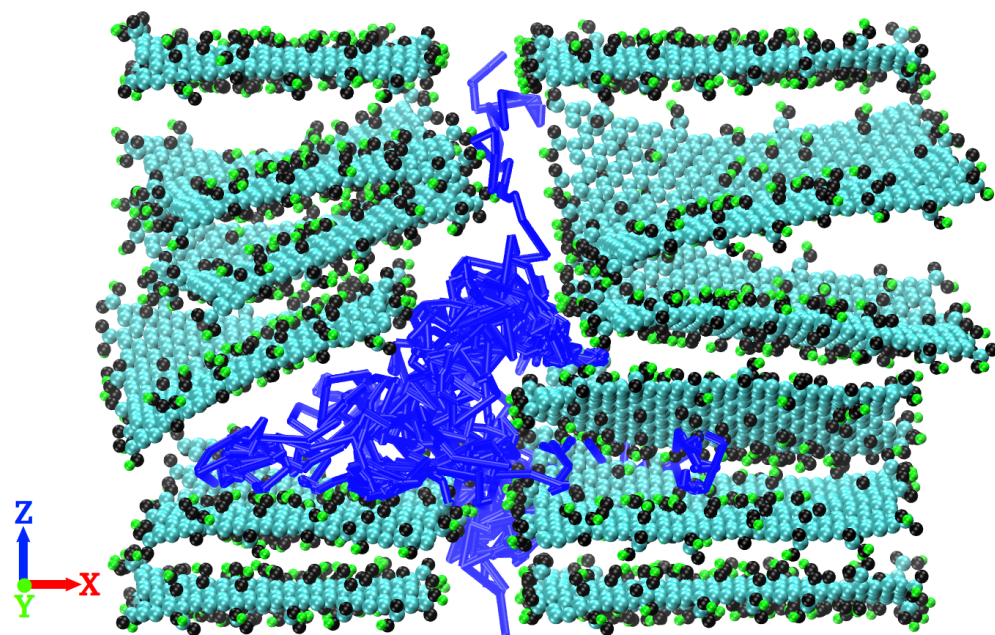


(a)

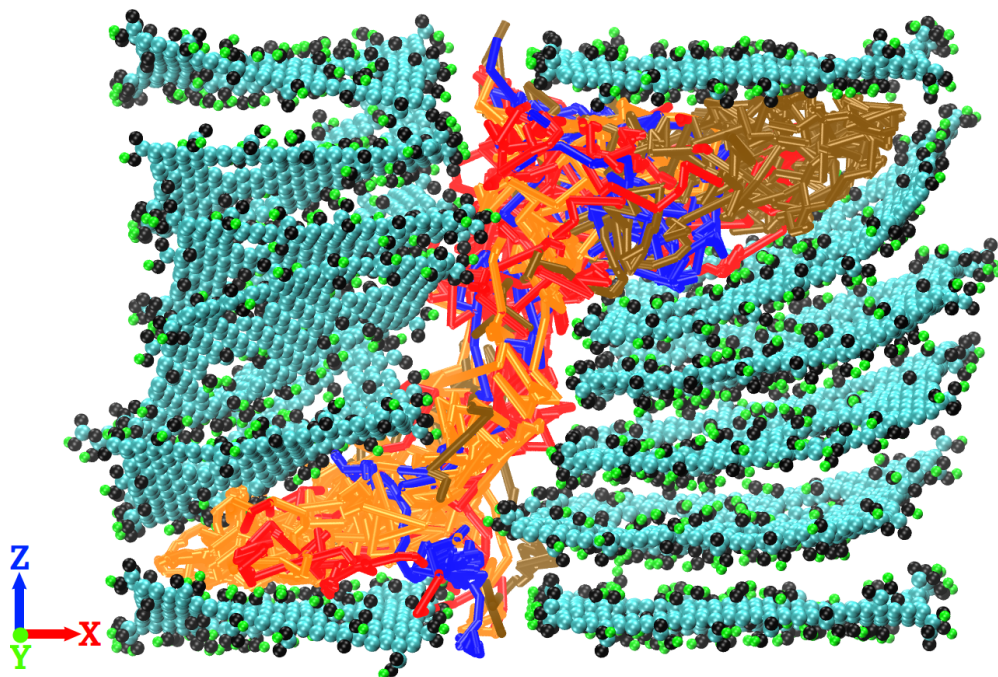


(b)

Fig. S14. Trajectory of Na^+ ions through layered GO membranes (a) 0-NP-IL, (b) 0-P-IL.



(a)



(b)

Fig. S15. Trajectory of Na^+ ions through layered GO membranes (a) 0-NP-nIL, (b) 0-P-nIL.

Distribution of permeation time and permeation velocity of the water molecules through the layered GO membranes

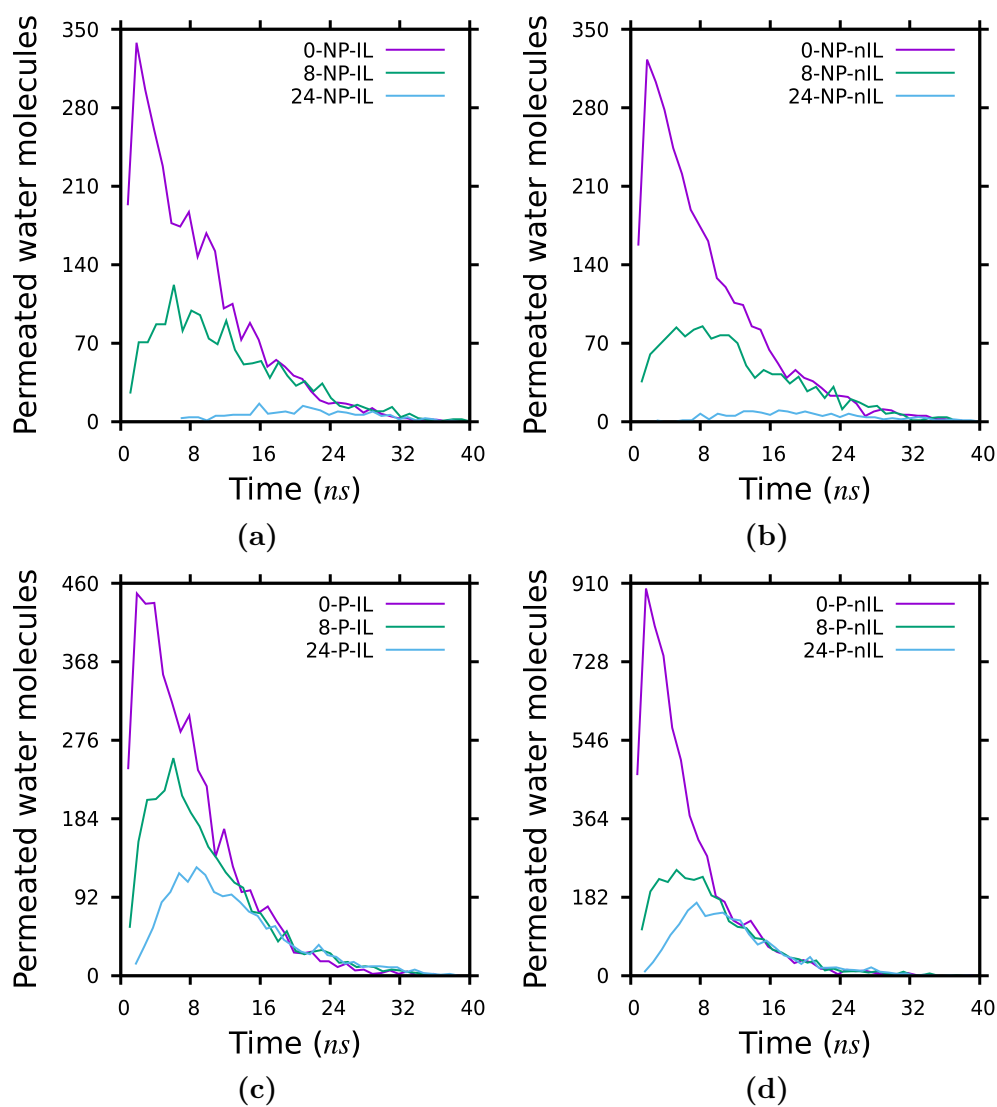


Fig. S16. Distribution of permeation time of the water molecules through the layered GO membranes. (a) No pinholes and ideal lamellar stacking. (b) No pinholes and non-ideal lamellar stacking. (c) Pinholes and ideal lamellar stacking. (d) Pinholes and non-ideal lamellar stacking.

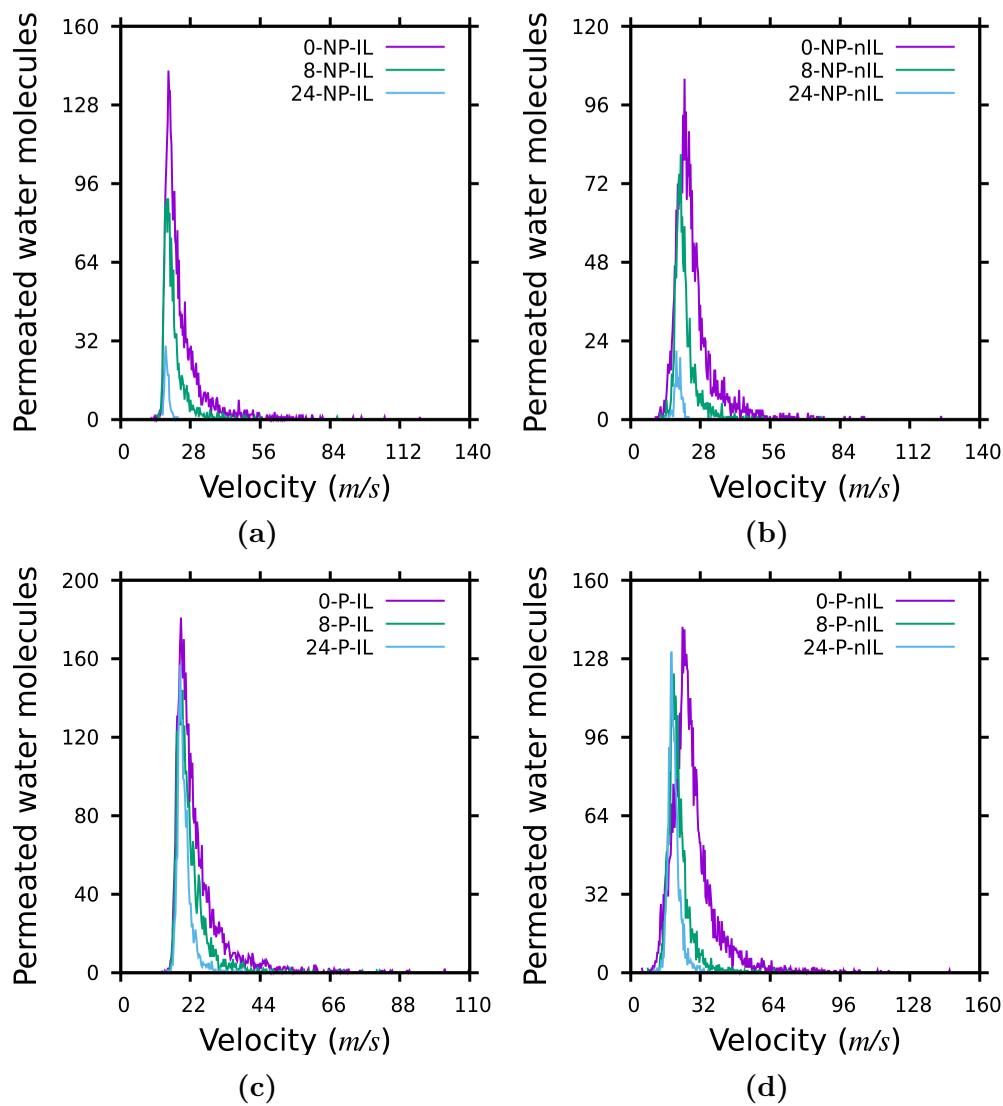


Fig. S17. Distribution of permeation velocity of the water molecules through the layered GO membranes. (a) No pinholes and ideal lamellar stacking. (b) No pinholes and non-ideal lamellar stacking. (c) Pinholes and ideal lamellar stacking. (d) Pinholes and non-ideal lamellar stacking.

Spatial distribution of water

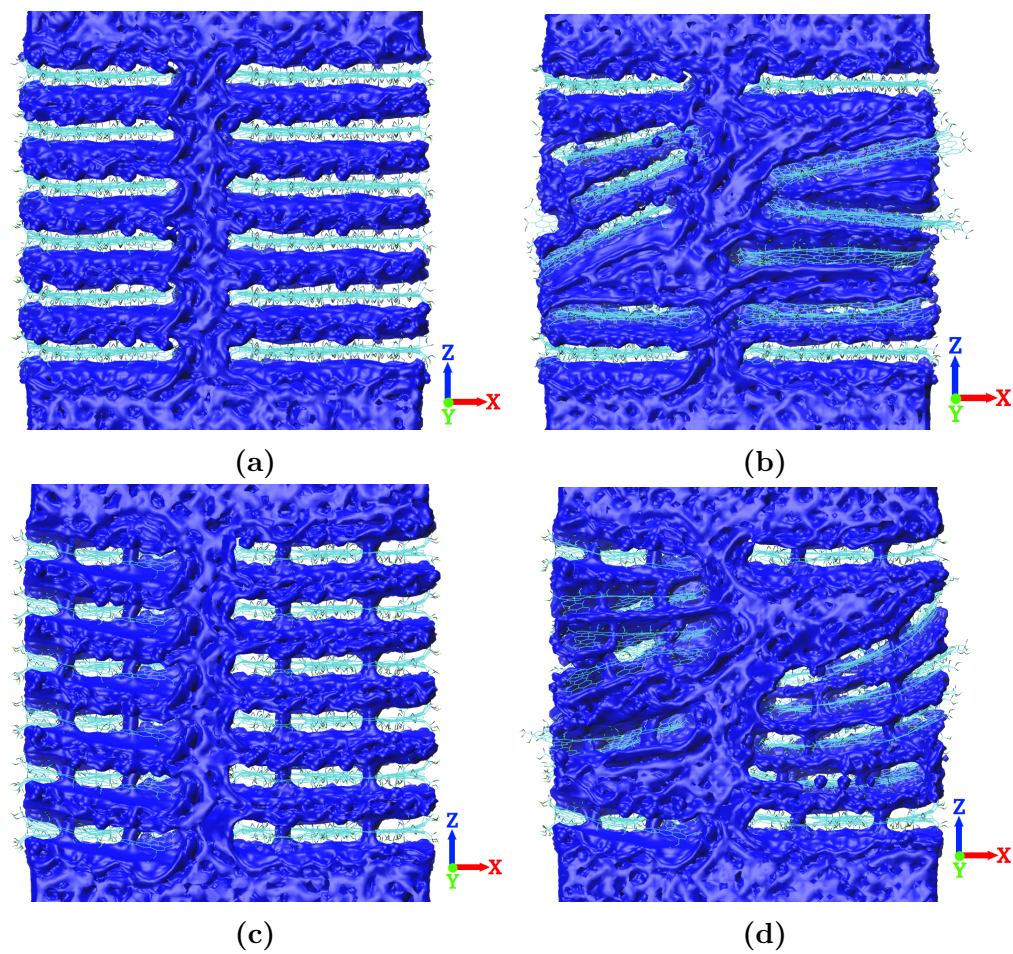


Fig. S18. Spatial distribution of water for layered GO membrane with $\mathbf{W} = 0.0 \text{ \AA}$. (a) 0-NP-IL. (b) 0-NP-nIL. (c) 0-P-IL. (d) 0-P-nIL.

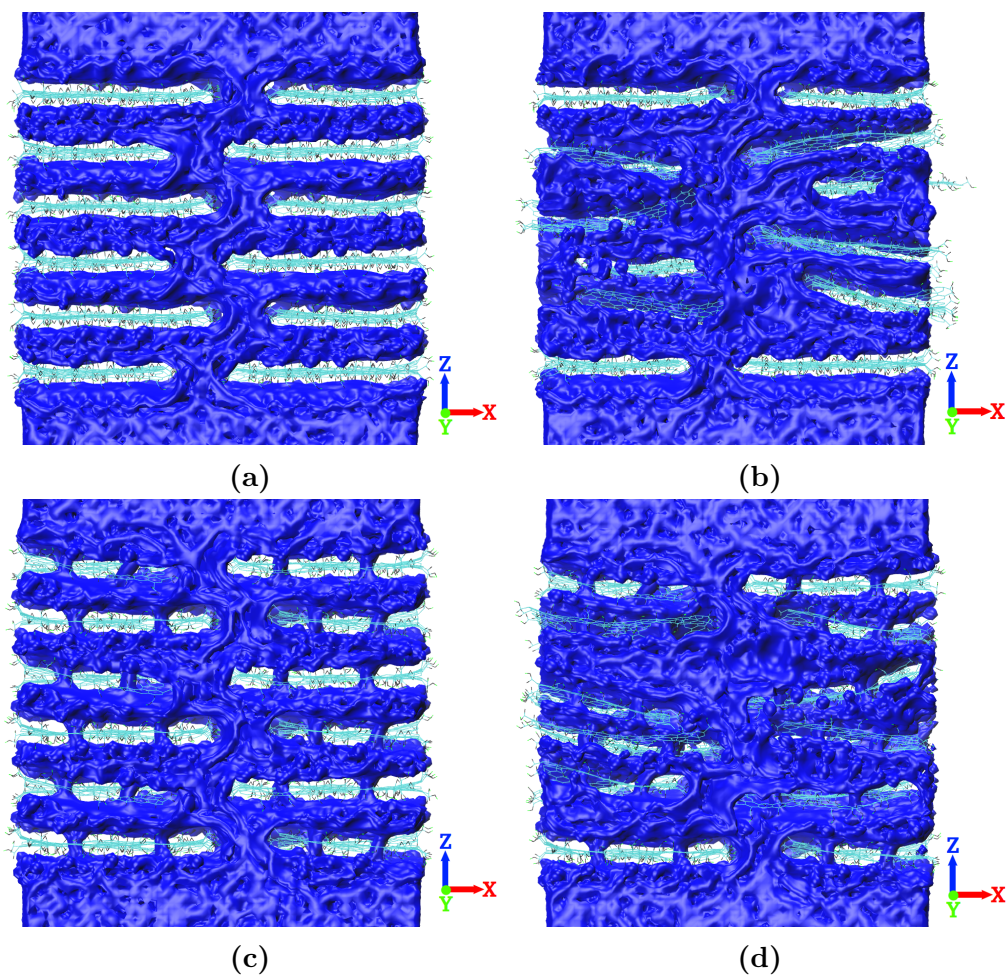


Fig. S19. Spatial distribution of water for layered GO membrane with $W = 8.0 \text{ \AA}$. (a) 8-NP-IL. (b) 8-NP-nIL. (c) 8-P-IL. (d) 8-P-nIL.

Variation of water flux with membrane thickness

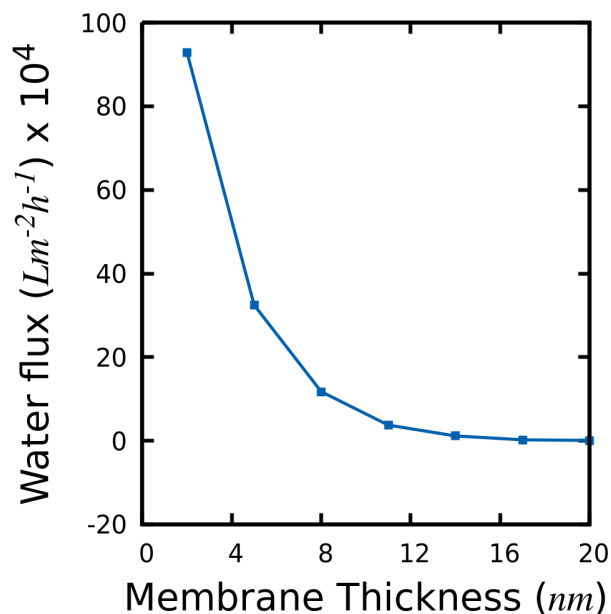


Fig. S20. Variation of water flux with the thickness of layered GO membrane (0-NP-IL configuration).

Table S2: Variation of water flux with membrane thickness (0-NP-IL configuration)

Membrane thickness (<i>nm</i>)	Water flux ($Lm^{-2}h^{-1}$) $\times 10^4$
2.0	92.782
5.0	32.447
8.0	11.747
11.0	3.743
14.0	1.165
17.0	0.237
20.0	0.082

To get some insight into the effect of membrane thickness on the water flux of layered GO membrane few additional simulations are performed for 0-NP-IL membrane configurations with different membrane thickness. As can be seen from Figure S20 and Table S2 with the increase in thickness the water flux through the layered GO membrane decreases.

Effect of number of pinhole defects on the performance of layered GO membrane

Table S3: Geometric configurations of the layered GO membrane considered for the study of effect of number of pinhole defects and their corresponding abbreviations

W (Å)	Geometric configuration of the membrane			Membrane abbreviations
	Pinhole defects	Lamellar stacking	Number of pinhole defects on a single layer of GO	
0.0	Yes	Ideal	4	0-P-IL-4N
0.0	Yes	Ideal	8	0-P-IL-8N
0.0	Yes	Ideal	12	0-P-IL-12N

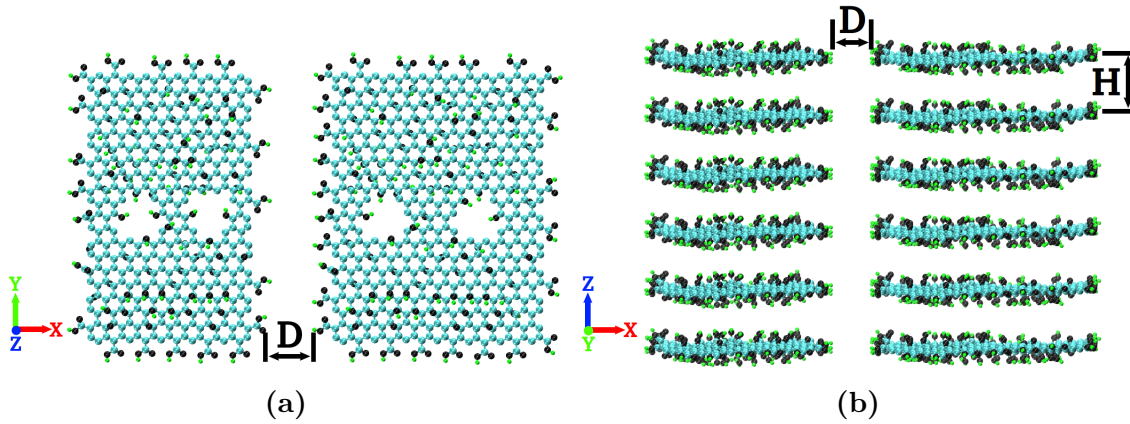


Fig. S21. Layered GO membrane with 0-P-IL-4N configuration. (a) Top view. (b) Side view. The green color is for hydrogen atoms, the black color is for oxygen atoms and the cyan color is for carbon atoms.

For investigating the effect of number of pinhole defects on the performance of layered GO membrane three different membrane configurations are considered. These membranes are abbreviated as 0-P-IL-4N, 0-P-IL-8N and 0-P-IL-12N. For 0-P-IL-4N configuration, 4 pinhole defects are considered on a single layer of the GO. Similarly, for 0-P-IL-8N and 0-P-IL-12N configurations 8 and 12 pinhole defects are considered on a single layer of GO respectively. The geometric configuration of these membranes considered for the study of effect of number of pinhole defects and their corresponding membrane abbreviations are shown in Table S3.

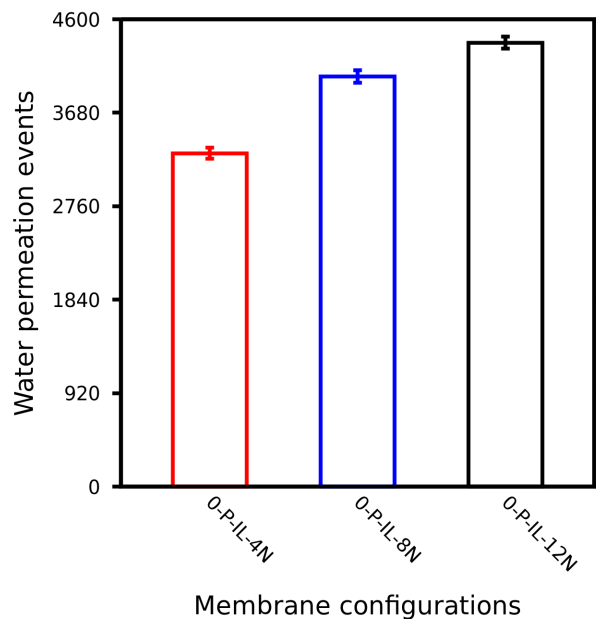


Fig. S22. Water permeability through layered GO membranes with different number of pinhole defects.

Figure S21 shows the structure of layered GO membrane with 0-P-IL-4N configuration.

For all these membrane configurations the value of the pore offset distance (**W**) is 0.0 Å and the GO nanosheets layers are perfectly aligned (i.e. they are parallel to each other). Similarly, the value of **D** is 7.0 Å and **H** is 10.0 Å for all these membranes.

The water permeability through the membranes with different number of pinhole defects is shown in Figure S22. As can be seen from Figure S22, with the increase in number of pinhole defects on the layered GO membranes, the water permeability through the membrane increases.

Effect of pinhole sizes on the performance of layered GO membrane

Table S4: Geometric configurations of the layered GO membrane considered for the study of effect of pinhole sizes and their corresponding abbreviations

W (Å)	Geometric configuration of the membrane			Membrane abbreviations
	Pinhole defects	Lamellar stacking	Effective diameter of pinhole defects (Å)	
0.0	Yes	Ideal	3	0-P-IL-3S
0.0	Yes	Ideal	5	0-P-IL-5S
0.0	Yes	Ideal	8	0-P-IL-8S

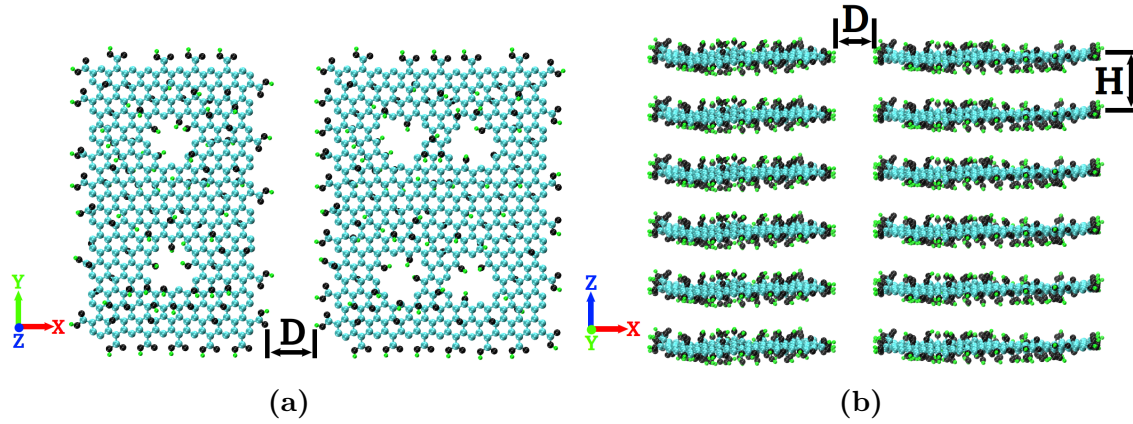


Fig. S23. Layered GO membrane with 0-P-IL-5S configuration. (a) Top view. (b) Side view. The green color is for hydrogen atoms, the black color is for oxygen atoms and the cyan color is for carbon atoms.

For investigating the effect of pinhole sizes on the performance of layered GO membrane three different membrane configurations are considered. These membranes are abbreviated as 0-P-IL-3S, 0-P-IL-5S and 0-P-IL-8S. For 0-P-IL-3S membrane configurations the effective diameter of the pinhole defects are 3 Å, for 0-P-IL-5S membrane configuration the effective diameter of the pinhole defects are 5 Å and for 0-P-IL-8S membrane configurations the effective diameter of the pinhole defects are 8 Å. The geometric configurations of the layered GO membranes considered for the study of effect of pinhole sizes and their corresponding

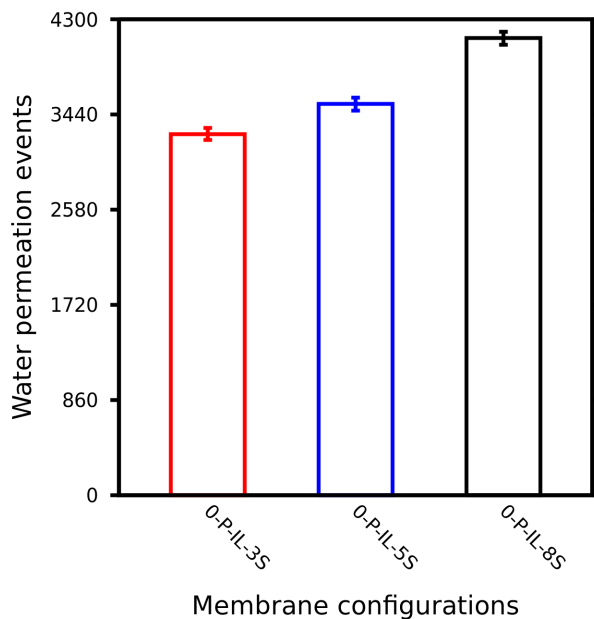


Fig. S24. Water permeability through layered GO membranes with different pinhole sizes.

membrane abbreviations are tabulated in Table S4. Figure S23 shows the structure of 0-P-IL-5S membrane configuration.

For all these membranes, there are 6 number of pinhole defects on a single layer of GO. The value of **D** is 7.0 Å and **H** is 10.0 Å for all these membranes. Similarly, the value of pore offset distance (**W**) of these membranes is 0.0 Å and the GO nanosheets of these membranes are perfectly aligned (i.e. parallel to each other).

The water permeability through layered GO membranes with different sizes of pinhole defects is shown in Figure S24. With the increase in sizes of the pinhole defects the water permeability through the layered GO membrane increases.

References

- (1) Jorgensen, W. L.; Maxwell, D. S.; Rives, J. T. *J. Am. Chem. Soc.* **1996**, *118*, 11225–11236.